

An analysis of the resilience capacity of soils in North China: a study on land subsidence treatment

Xiu-yan Wang · Lin Sun · Zhi-liang Wang ·
Chang-li Liu · Yun Zhang

Received: 17 August 2012 / Accepted: 26 November 2013 / Published online: 17 December 2013
© Springer-Verlag Berlin Heidelberg 2013

Abstract In order to study treatment measures for the land subsidence caused by deep groundwater overexploitation, we conducted soil compression and rebound tests to analyze the unloading and rebound regularity of deep soil on the fringes of three typical land subsidence regions in North China. Using fuzzy mathematics, we specifically explored the main factors influencing the soil mass unloading resiliency. The results indicated that the ratio between the unloading resilience volume and the loading deformation volume of soil mass in the study areas (referred to as the resilience capacity of soil mass) is between 1.6 and 37.6 %, with an average of 14.7 %. In other words, only about 14.7 % of the land subsidence deformation in the study areas can be restored. The soil masses with different properties in North China all possess elastoplasticity and the resilience capacities of soil can vary from area to area. The sandy soil is not completely elastic but has a certain degree of plasticity; the resilience capacity of soil mass is not a constant, but rather, a variable that changes with the rebound stress value. When the rebounding stress value is determined, the resilience capacity under a smaller unloading stress is larger than that under a larger unloading stress, which demonstrates that earlier land subsidence treatment can result in better effects. Meanwhile, the resilience capacity of soil mass is also enhanced with the increase of rebounding stress, indicating that the closer to the original groundwater level the restored groundwater is, the better the resilience capacity will be. After repeated loading and unloading tests have been conducted under the same stress, the resilience

capacity of soil mass will, in most cases, increase to a certain extent. These results can be quite conducive to the treatment of deep groundwater exploitation-induced disasters such as land subsidence.

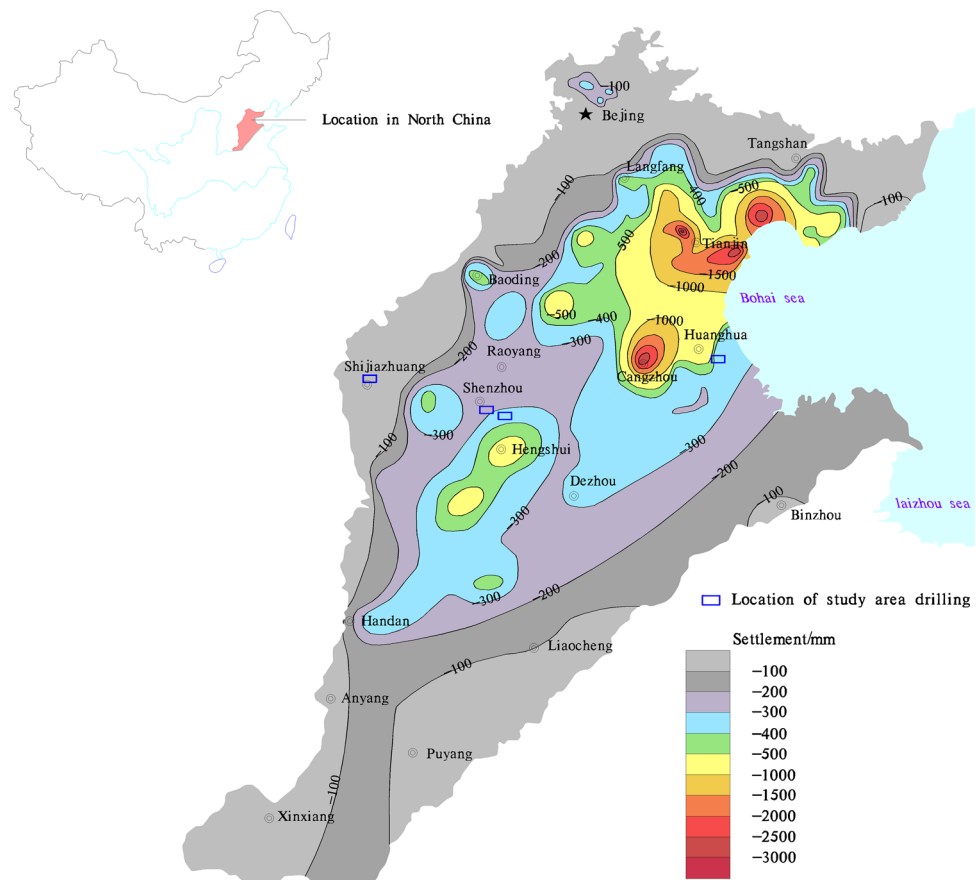
Keywords Soil unloading rebound · Resilience capacity · Deep groundwater overexploitation · Controlling subsidence · North China

Introduction

North China is located in a temperate zone with a semi-arid and subhumid climate, in which the annual average evaporation far exceeds precipitation, and deep groundwater is the main water source for local industrial, agricultural, and domestic uses because of the severe scarcity of surface fresh water. The deteriorating trend of land subsidence and its concomitant disasters (Teatini et al. 2005; Hu 2004; Sakiyan and Yazicigil 2004) caused by deep groundwater exploitation have resulted in the formation of depression cones in North China, which are unique to the rest of the world. They have triggered huge economic losses and impaired the natural environment and sustainable development of the economy and society, making the case for urgent attention and treatment to this issue.

The most effective way of tackling land subsidence is to restore the groundwater funnel and elevate the water level so as to make the soil mass rebound (Adrian et al. 1999; Shi et al. 2008; Lubis et al. 2011). However, there is still a lack of research data on how and when to take these measures to effectively enhance the resilience capacity of the soil mass. Therefore, it is of great necessity to study the unloading resilience properties of soil mass within the

X. Wang (✉) · L. Sun · Z. Wang · C. Liu · Y. Zhang
Institute of Hydrogeology and Environmental Geology, Chinese Academy of Geological Sciences, Shijiazhuang 050061, China
e-mail: Wxiuyan9948@163.com

Fig. 1 Location of study area

influencing depths of groundwater exploitation in North China, in order to provide scientific parameters for geological disaster control and response.

Compressive deformation occurs when the soil mass is loaded, whereas the soil mass rebounds when unloaded. However, the soil mass is not an ideal elastic object, and different deformation exists in the soils with different properties when loaded and unloaded. It has been basically acknowledged in the previous studies that cohesive soil is elastoplastic. Part of the deformation of the cohesive soil can be recovered after unloading, which is called elastic deformation, while part of the deformation can not be restored, known as plastic deformation. However, controversies exist on the deformation of sandy soil. Traditionally, it has been considered that the compression of sandy soil is instantaneous, elastic, restorable, and completely elastic per se, i.e., the deformation can be recovered completely after unloading. However, some new viewpoints hold that sandy soil is also elastoplastic (Zhang et al. 2010; Liu et al. 2004). Some research has been made on the unloading resilience of shallow soil, and made a number of research results (Zhuang and Xie 2005a, b; Jia et al. 2009; Wu et al. 2010), but research on the unloading resilience properties of the soil in North China, particularly the deep soil, is rare.

Test

As is shown in Fig. 1, the study site is located in the fringes of a typical land subsidence area caused by groundwater exploitation in North China. Figure 1 was drawn based on the land subsidence map of the North China Plain (2002 version). Test samples were taken from five boreholes in three land subsidence areas of Cangzhou, Hengshui, and Shijiazhuang, of which Cangzhou had one borehole, and the other two regions had two boreholes, respectively. Since the two boreholes in Hengshui were 15 km away from each other with different stratum structures, they were counted as two independent boreholes. The two boreholes in Shijiazhuang were no more than 500 m away from each other with similar stratum structures, so they were counted as one borehole. As was revealed by the drilling, the stratum mainly consists of Quaternary, alluvial-proluvial materials. There are mainly five kinds of soil properties: clay, silty clay, silt, fine sand, and medium coarse sand. Based on the influencing depth range of deep groundwater exploitation, the maximum soil depth in this study is about 500 m.

The uniaxial compression test was adopted as the main test method in this study, supported by such tests as specific gravity, density, water content, particle analysis, and the

lateral pressure test method. Two kinds of instruments were used in the uniaxial compression test, including: (1) The automatic high-pressure consolidometer produced by Beijing Huakan Technology Co., Ltd., which possesses a measuring range of 3.2 MPa and is suitable for samples with burying depth <100 m; and (2) a multi-functional, automated consolidation, combined permeameter that we designed with vertical stress and lateral stress, pore-water pressure, and vertical deformation, capable of measuring the greatest range of 20 MPa, which is suitable for samples with burying depth >100 m (Wang et al. 2011). Given that most of the soil samples in the study area are deeply buried with great hardness and slight deformation, the criterion to determine whether the deformation is stable or not is a degree of no larger than 0.005 mm/h in the compression test, which is more accurate than the national standard of 0.01 mm/h for soil testing (standard for soil test method, 1999).

It is generally believed that the soil samples, after being extracted (Di Prisco et al. 2000), are relieved of the gravity pressure of the overlying soil under natural conditions. By taking into account the fact that the groundwater level has dropped by approximate 50 m (a 10-m drop in the water level is equivalent to an increase of approximately 100 kPa in stress to the soil) in most urban areas in North China, the repeated loading and unloading tests need to be conducted with a unloading stress of about 400 kPa within a range of stress P_0+600 kPa.

Soil resilience takes place on the basis of compressive deformation, therefore, the following three indicators of the soil compression resilience index (the Writing Committee 1993) and resilience capacity are used to describe the properties of soil resilience.

(1) Compression index (C_c):

$$\text{Expression: } C_c = (e_i - e_{i+1}) / (\text{Lgp}_{i+1} - \text{Lgp}_i). \quad (1)$$

C_c is the compression index, which is dimensionless; e_i and e_{i+1} represent the dimensionless void ratio on the straight line of the e-lgP curve when the stress values are P_i and P_{i+1} ; P_i and P_{i+1} stand for the stress values corresponding to e_i and e_{i+1} , respectively (unit: kPa). As a constant value, the compression index C_c is the slope of the linear part of the compression test e-lgP curve, and is a fixed value that does not change with increasing stress. The bigger the compression index is, the higher plasticity the soil mass will have, which can bring about heavier land subsidence.

(2) Rebound index (C_s):

$$\text{Expression: } C_s = (e'_i - e_{i+1}) / (\text{lgp}_{i+1} - \text{Lgp}_i). \quad (2)$$

where C_s is the resilience index, dimensionless; e_{i+1} , e_i represent the dimensionless void ratio that the stress from p_{i+1} rebound to stress P_i . The resilience index is the slope

of the linear part of the hysteresis loop on the resilience test e-lg p curve. It's deemed as a variable that is subject to the influence of both soil mass properties and rebounding stress. The greater the resilience index value is, the heavier deformation the soil mass will have. The compression index and resilience index share the same equation, and the way of differentiating them is to judge whether parameters in the compression phase or in the resilience phase are used.

The land subsidence treatment effects can be reflected by the range of soil mass resilience. By inserting the void ratio (under a certain degree of stress) formula $e_i = (1+e_0)(h_i/h_0) - 1$ into formulas (1) and (2), we can obtain the following formula:

$$C_s/C_c = (h'_i - h_{i+1}) / (h_i - h_{i+1}) = \Delta h_{i+1} / \Delta h_i, \quad (3)$$

where h_i stands for the height of a sample after the deformation becomes stabilized, h'_i stands for the height of a sample after the resilience becomes stabilized, h'_i , h_i (unit: mm). This formula actually represents the ratio value between the resilience deformation and compression deformation of the soil mass, which reflects the range of the soil mass resilience and is adopted in this paper to express the resilience capacity of the soil mass.

Analysis of test results

Resilience properties in different regions

As most of the soil samples are deeply buried and hard in property, the ratio value between the resilience index and the compression index of the soil sample in a certain region (C_s/C_c) doesn't vary significantly, with the resilience capacity ranging from 1.63 to 37.61 %. However, the value of C_s/C_c in different regions varies a bit, which indicates regional differences. The soil resilience capacity (C_s/C_c) in different regions and variation characteristics of related parameters are shown in Table 1, where the resilience capacity is the average value gained from at least two resilience tests. Figure 3 shows the variation of resilience parameters with the changes of buried depth. In order to display the resilience capacity of the sand soil in the figure, the plastic index of the sand is assumed to be 0. As is seen from Table 1 and Fig. 2, the soil mass in the Hengshui-1 area, which contains a large amount of moisture and is relatively soft in property, has the smallest resilience capacity (C_s/C_c). The soil mass in Huanghua has the strongest resilience capacity, followed by Shijiazhuang and Hengshui.

Figure 3 indicates that the soil resilience capacity tends to be strengthened with the increase of burial depth (h/m); however, the variation tendency is not so obvious in the Hengshui-1 area.

Table 1 Statistics of compression parameters in different regions

Experiments program	Site Number of samples	Huanghua 18	Hengshui-1 17	Hengshui-2 17	Shijiazhuang 34
Rebound index/Compression index $C_s/C_c/\%$	Minimum	9.778	1.630	6.415	10.06
	Maximum	37.607	16.518	26.136	28.22
	Average	20.893	6.636	15.129	15.88
Compression index/ C_c	Minimum	0.104	0.145	0.027	0.051
	Maximum	0.311	0.404	0.145	0.217
	Average	0.172	0.207	0.077	0.114
Resilience index/ C_s	Minimum	0.021	0.003	0.006	0.007
	Maximum	0.056	0.047	0.017	0.041
	Average	0.033	0.015	0.010	0.018
Water content/ $\omega/\%$	Minimum	16.50	17.64	6.20	5.60
	Maximum	27.40	44.40	22.4	29.34
	Average	20.30	24.34	14.00	17.37
Void ratio/ e	Minimum	0.471	0.506	0.441	0.460
	Maximum	0.718	1.355	0.525	0.880
	Average	0.574	0.704	0.490	0.581
Plasticity index/ I_p^*	Minimum	14.46	8.5	9.4	4.5
	Maximum	22.96	21.5	18.4	22.8
	Average	17.4	14.9	13.4	10.9
Liquidity index/ I_L^*	Minimum	-0.22	-0.13	-0.96	-0.98
	Maximum	0.45	1.25	0.04	0.30
	Average	0.02	0.28	-0.42	-0.17

* Project does not include sandy soil

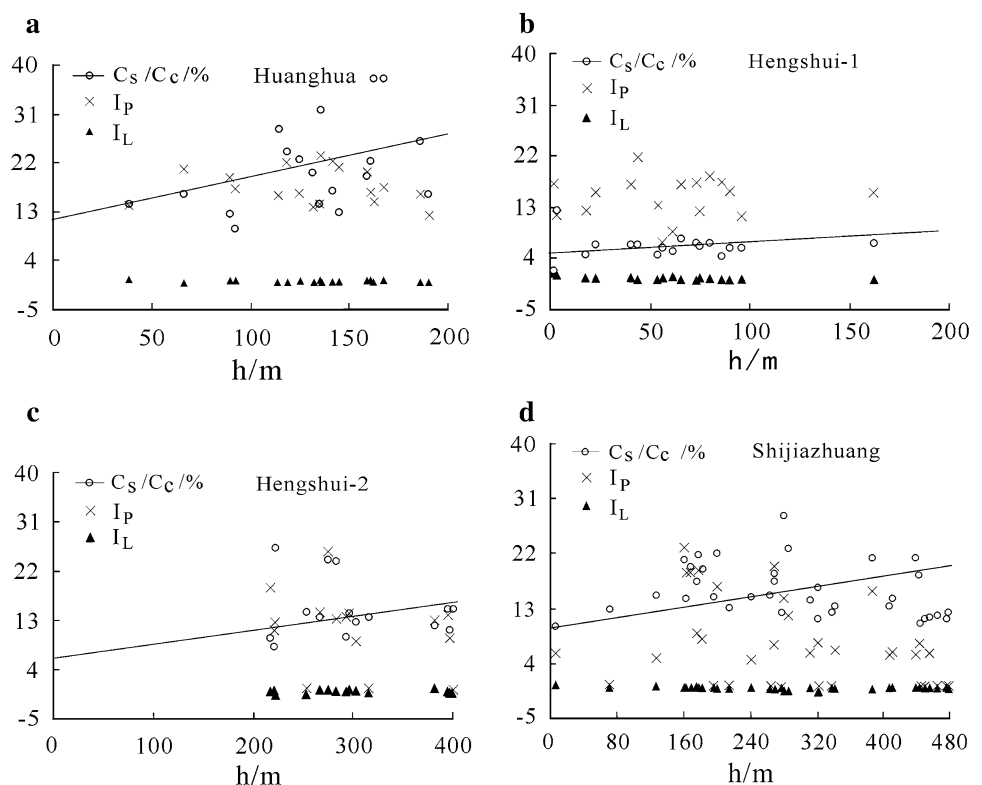
Fig. 2 The characteristics of unloading rebound in different areas

Fig. 3 Curves of the rebound characteristics in different soils

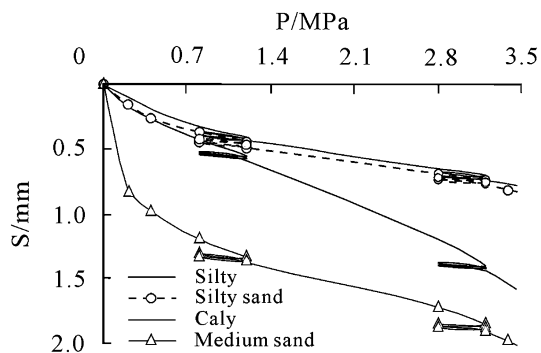
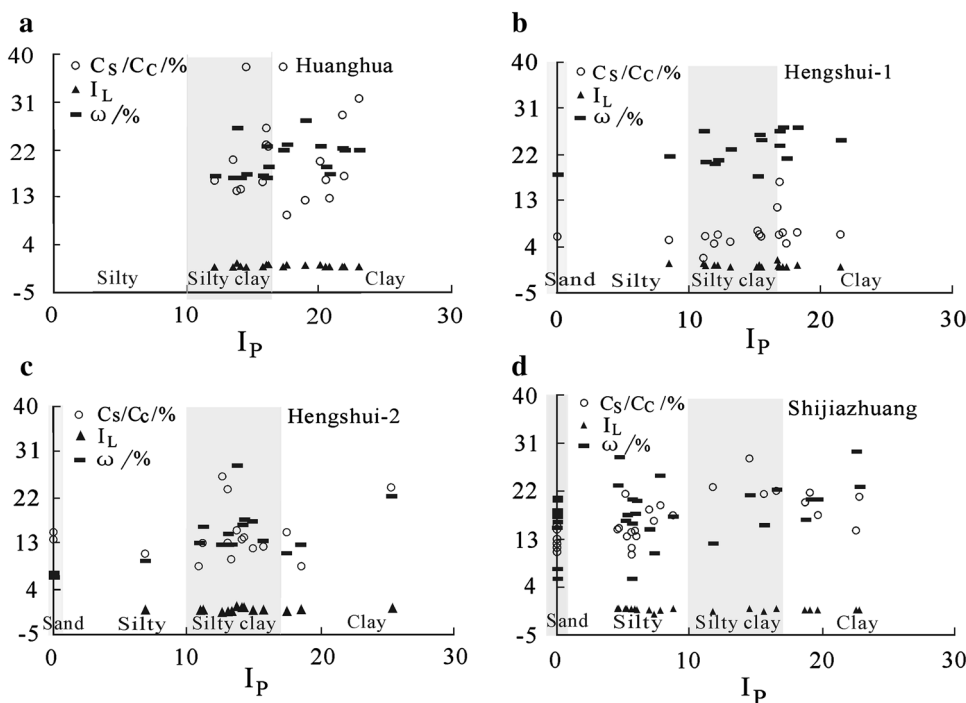


Fig. 4 Curves of deformation and rebound in different soils

Resilience of the soils with different properties

Test results show that the soil mass is not so cohesive in the study areas with a general plasticity index I_p of less than 30. For the soil samples in the same area (Fig. 3), those with relatively strong resilience capacity (C_s/C_c) include the silty clay with a plasticity index (I_p) between 10.5 and 16.7, the clay with a plasticity index (I_p) between 17.1 and 25.3, and a small amount of silt (e.g., in Shijiazhuang) with an I_p between 7.0 and 9.0, while those with relatively small resilience capacity include fine sand, silty sand, and calcareous-cemented soil. The resilience capacities of the soils with different properties in different regions are shown in Figs. 3, 4. Figure 4 shows the deformation resilience curve of the soil samples at similar burial depths under different stresses in the same region, revealing that

the resilience capacity is similar between the silt and silty sand, but that of the cohesive soil shows a relatively obvious variation.

It is worth mentioning that the soil rebounds only when additional stress is less than the critical bearing capacity to rebound primarily by the elasticity (Wang et al. 2003). The test results have proved that sandy soil is not the kind of soil with complete elasticity, as was thought previously. Being elastoplastic, its resilience capacity is smaller than the local average resilience capacity in most cases.

Under the influence of repeated loading and unloading, the resilience capacity increment of the sand, up to 33%, is greater than that of the cohesive soil. However, complete elasticity could not be achieved by the sand with repeated loading and unloading. On the other hand, the resilience capacity of the calcareous-cemented soil does not change much.

Relationship between unloading resilience capacity and the stress of soil mass

By allowing for geological-environmental hazards caused by groundwater exploitation, we conducted repeated loading and unloading tests on soil samples under different stresses. Three unloading tests under stresses ranging from 1,200 to 400 kPa showed that in line with the continuously increasing stresses for the same soil sample, the unloading resilience capacities under different degrees of stress varied a bit, and the unloading resilience capacity with a smaller degree of stress was greater than that under a heavier stress.

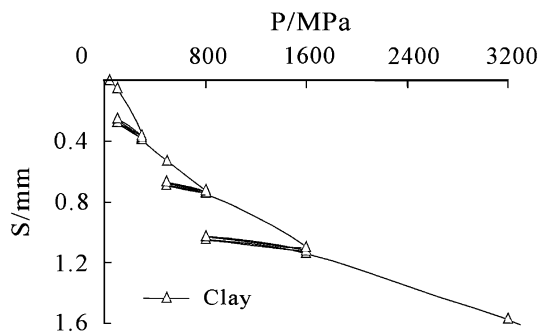


Fig. 5 Curves of unloading-rebound in different stress conditions

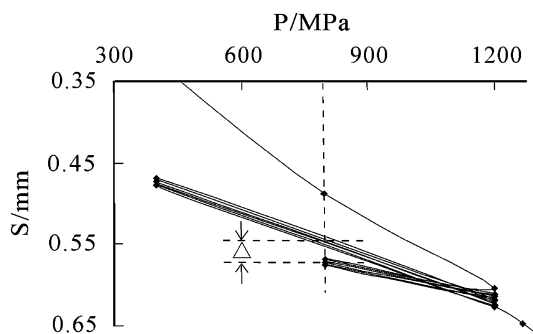


Fig. 6 Curves of unloading in different stress conditions at the same stress point

As shown in Fig. 5, the unloading resilience capacities (C_s/C_c) were 10.03, 6.39, and 6.07%, respectively, under the stresses of 300, 800, and 1,600 kPa. However, if unloaded at the same stress point, the larger the unloading stress is, the greater resilience capacity the soil will have. As shown in Fig. 6, the resilience capacities of the samples were 32.27 and 52.37%, respectively, under the stresses from 1,200 to 800 kPa and from 1,200 kPa to 400 kPa. Although the increment of resilience capacity of the soil samples with different properties in different regions varies, the resilience capacities of all soils with different properties in the study areas were seen to increase (namely, clay and sand soils), indicating that earlier treatments of land subsidence can be more effective since a greater degree of groundwater restoration brings about higher resilience capacity.

Main factors influencing resilience capacity

The resilience capacity is affected by many factors, among which the physical mechanical property of the soil mass is conceived to be the most influential. However, the question of which factor has a greater impact on the resilience capacity remains to be answered. In our study, the Gray correlation method of the grey system theory (Liu and Lin 2011) was employed to analyze the effect of physical

mechanical indexes of soil mass on resilience capacity. Specific procedures are as follows:

1. Determination of reference sequence and comparison sequence

The soil resilience capacity value and 13 physical mechanical property indices were selected as the criteria for the reference sequence determination, including burial depth (h/m), gravity (G), density (ρ), water content ($w/\%$), void ratio (e), plasticity index (I_p), liquid index (I_L), content of sand particles (particle diameter $\Phi > 0.075$), content of silt particles ($0.005 < \Phi \leq 0.075$), content of clay particles ($\Phi \leq 0.005$), compressibility coefficient (a), compression modulus (E), resilience index (c_s), compression index (c_c), and lateral stress k_0 . Reference sequence numbers were defined respectively as $x_1, x_2, x_3, \dots, x_{13}$. Parameters at different depths constituted a separate line and parameters in one region constituted a sequence, thus formulating four sets of sequences, namely Huanghua, Hengshui-1, Hengshui-2, and Shijiazhuang, which contain 18 groups, 17 groups, 17 groups, and 34 groups, respectively. Then the Hengshui-1 sequence was put into Table 2 as a representative. Furthermore, since some of the parameters are variables that change with stress, the lateral stress parameters in Table 2 have all adopted the average under-stress values of $p_0 + 0.6$ MPa based on the conditions of groundwater exploitation in the study areas, and the resilience parameter has adopted the average under-stress values of about 400 kPa within a range of stress $< P_0 + 600$ kPa (equivalent to the groundwater level dropping 60 m, then rising 40 m)

2. Correlation analysis

1. Dimensionless treatment was performed on the data by virtue of initialization. All data in each sequence divided by the first number of each sequence can yield a new set of sequences, and then the numbers of the first line of each sequence will all be 1.
2. The difference sequence: After initialization, if we subtract the first number from the numbers in each line and take the absolute value by dint of the formula $\Delta_i(k) = |x_i(K) - x_0(k)|$, then we can get another data sequence, which is shown in Table 2; i is the number of rows ($i = 1-17$), k is the number of columns ($k = 0-13$). The first column of the new data sequence is all 0, in other words, it is a column fewer than the original sequence. Then, the maximum and minimum numbers in each column are separately picked out and listed as two separate lines of data, respectively.

Table 2 Soil sample physical mechanical properties in Hengshui-1 area

Lithology	Cs/ Cc/%	Dpth/ h/m	Gravity/ G	Density/ ρ/cm^3	Water content/W/ %	Void ratio/e	Plasticity index/ I_p	Liquid index/ I_L	$\phi > 0.075/$ %	$0.005 < \phi \leq$ $0.075/$ %	$\phi \leq 0.005$ /%	*Resilience index/ C_s	*Compression index/ C_c	*Lateral stress/ K_0
	x0	x1	x2	x3	x4	x5	x6	x7	x8	x9	x11	x11	x12	x13
Silty clay	11.63	1.70	2.73	1.67	44.4	1.355	16.7	1.25	4.5	42.7	52.8	0.047	0.404	0.370
Silty clay	1.63	2.20	2.72	1.77	26.5	0.941	11.1	0.82	7.5	56.6	35.9	0.003	0.184	0.200
Silty clay	4.74	17.70	2.72	2.09	20.3	0.567	12.0	0.24	6.5	55.3	38.2	0.009	0.190	0.156
Silty clay	6.40	22.64	2.73	2.04	25.9	0.683	15.3	0.18	8.8	57.7	33.5	0.011	0.172	0.180
Silty clay	6.48	40.70	2.73	1.98	26.5	0.743	16.9	0.29	4.9	48.5	46.6	0.016	0.247	0.200
Clay	6.45	44.20	2.75	2.07	24.9	0.662	21.5	0.06	0.0	43.5	56.5	0.014	0.217	0.250
Silty clay	4.80	53.80	2.72	2.00	22.9	0.667	13.2	-0.04	4.5	55.1	40.4	0.011	0.229	0.215
Silty sand	5.92	56.90	2.69	1.88	18.0	0.685			50.8	47.8	1.4	0.009	0.152	0.170
Silty	5.19	61.20	2.71	2.05	21.6	0.610	8.5	0.66	26.1	67.1	6.8	0.008	0.154	0.180
Silty clay	16.52	65.00	2.73	2.05	23.6	0.650	16.9	0.10	5.0	41.3	53.7	0.037	0.224	0.200
Clay	6.64	73.70	2.74	2.01	27.1	0.732	17.1	0.10	3.1	40.4	56.5	0.015	0.226	0.241
Silty clay	6.29	74.90	2.72	2.09	21.0	0.610	12.1	0.37	6.4	42.5	51.1	0.011	0.175	0.250
Clay	6.75	80.10	2.74	2.05	27.1	0.648	18.3	0.20	1.8	43.1	55.1	0.017	0.252	0.320
Clay	4.48	85.53	2.74	2.11	21.3	0.732	17.3	0.04	4.8	41.3	53.9	0.009	0.201	0.380
Silty clay	6.00	89.90	2.73	1.96	24.9	0.573	15.5	0.00	7.5	45.3	47.2	0.012	0.200	0.230
Silty clay	6.00	96.30	2.72	2.07	20.5	0.698	11.2	0.26	8.6	63.1	28.3	0.009	0.150	0.35
Silty clay	6.90	162.40	2.73	2.13	17.6	0.573	15.2	-0.13	6.2	46.1	47.7	0.010	0.145	0.46
Correlation degree		0.620	0.494	0.445	0.831	0.847	0.539	0.647	0.829	0.503	0.518	0.578	0.801	0.711

ϕ is the soil particle diameter

* The value indicated is the average under-stress value of the $p_0 + 0.6 \text{ MPa}$

3. Establishing a data sequence of correlation coefficients:

Based on the sequence in 2, a data sequence of correlation coefficients could be set up, the formula for which is as follows:

$$\xi_i(K) = \frac{\min_i \min_k \Delta_i(k) + \zeta \max_i \max_k \Delta_i(k)}{\Delta_i(K) + \zeta \max_i \max_k \Delta_i(k)}. \quad (4)$$

In this formula, $i = 1-17$, $k = 0-13$, and ζ is the resilience index. According to the empirical correlation formula, ζ is set at 0.5 ($\zeta = 0.5$). Then the data sequence of correlation coefficients can be obtained based on the formula (4).

4. Calculating the degree of correlation:

The correlation degree of the data sequence 3 can be calculated by virtue of the mean value method with the following:

$$\text{formula } r_i = \frac{1}{n} \sum_{k=1}^n \xi_i(k). \quad (5)$$

In this formula, $n = 17$ and r_i represents the correlation degree between x_0 and x_i . A higher value of r_i indicates closer correlation between x_0 and x_i . Based on formula (5), the correlation degrees obtained are as follows: $r_1 = 0.620$, $r_2 = 0.494$, $r_3 = 0.445$, $r_4 = 0.831$, $r_5 = 0.847$, $r_6 = 0.539$, $r_7 = 0.647$, $r_8 = 0.829$, $r_9 = 0.503$, $r_{10} = 0.518$, $r_{11} = 0.578$, $r_{12} = 0.801$, and $r_{13} = 0.711$. The correlation degree ranks as $R_{12} > R_5 > R_3 > R_5$, indicating that the R_{12} and r_5 and r_3 and r_5 have closer correlation with the reference sequence. Correlation calculations are shown in Table 2. The correlation degree ranks indicate that the void ratio (e), the water content ($w/\%$), the content of sand particles (particle diameter $\Phi > 0.075$), the compression index (c_c), the lateral stress k_0 , the liquid index (I_L), the burial depth (h/m), the resilience index (c_s), the plasticity index (I_p), and the content of sand particles ($\Phi \leq 0.005/\%$) have closer correlation to the reference sequence (c_s/c_c). The correlation degree is more than 0.51.

Analysis and discussion

Testing results demonstrate that for the deep soil mass in North China under a small unloading stress (e.g., between 100 and 200 kPa), the resilience of soil mass is not significant, and even the deformation would continue to be enlarged merely from the increasing rate of deformation slowing down a bit. This might indicate that the unloading stress in the study has not exceeded the stress value derived from the seasonal water level variation, while the loading stress imposed on the soil mass is relatively heavier, thus causing deformation to continue in the soil mass. It might

also imply that the intensity of land subsidence (Zhang et al. 2010) treatment should not be too small; for example, the recharged water level should at least exceed the average variation amplitude of the multi-year, seasonal water level.

During the repeated loading and unloading tests on the soil samples, the resilience capacity increased in most circumstances, especially for sandy soil, of which the resilience capacity increased significantly. If time for the resilience of the soil mass was sufficient, the resilience capacity would have increased further. However, the resilience capacity of the soil mass would not increase without limits, because even with the repeated loading and unloading under the same loading volume, the deformation of the soil mass would also increase, a fact that has been proven by this test, as well as by the repeated loading and unloading tests conducted previously. Some irreversible plastic deformations have permanently been included in the soil mass deformation (Garlanger 1972). The sand soil in North China is not completely elastic. The sand would be quickly stabilized after deformation with either loading subsidence or unloading resilience, which is directly related to the great permeability of the sand. Similar results are also revealed by studies in other regions (VLade and Liu 1998; Zhang et al. 2010; Shamoto et al. 1997; Oda and Kazama 1998).

Constrained by the drilling methods, the sandy soil samples are more easily disturbed and difficult to collect compared with the cohesive soil samples. These factors might have influenced the testing results. However, through large quantities of tests, the basic resilience properties of North China can still be reflected.

Conclusions

Based on compression tests over the deep soil in different sites of North China, the following conclusions can be drawn:

1. The resilience capacity of soil mass is a variable, the unloading stress is a constant, and the unloading resilience capacity of soil mass under a smaller stress was greater than that under a heavier stress. When unloaded at a fixed stress point, the greater the unloading stress was, the greater the resilience capacity would be. The soils with different properties in the study areas have all shown this kind of characteristic, demonstrating that the timing and intensity of land subsidence treatment need to be adequately considered. Earlier treatment can lead to larger degree of water level restoration (at least, the recharged water level should, at minimum, exceed the average

- variation amplitude of multi-year seasonal water level) and higher resilience capacity, and result in more effective treatment.
- The soil mass is elastoplastic. Test results show that the resilience capacity (C_r/C_c) ranges between 1.63 and 37.6 % in the study areas with an average of 14.7 %. The sand is not completely elastic, and its resilience capacity is generally lower than that of the clay, however, under the influence of repeated loading and unloading, the resilience capacity increment of the sand was much higher than that of the clay. The sand is still elastoplastic even after unlimited repetitions of loading or unloading.
 - Regarding the combination of factors that impact the soils, as is indicated by the grey system theory, the soil mass resilience capacity is primarily influenced by the void ratio (e), the water content ($w/\%$), the content of sand particles (particle diameter $\Phi > 0.075$), the compression index (c_c), the lateral stress k_0 , the liquid index (I_L), the burial depth (h/m), the resilience index (c_s), the plasticity index (I_p), and the content of clay particles ($\Phi \leq 0.005$ %), with a correlation degree more than 0.51. Regarding soil consistency, the soils with relatively higher resilience capacity mainly include the silty clay with the plasticity index (I_p) between 10.5 and 16.7, the clay with the plasticity index (I_p) between 17.1 and 25.3, and a small amount of silt with I_p between 7.0 and 9.0, while those with relatively lower resilience capacity include fine sand, silt sand, and calcareous-cemented soil.
 - The resilience capacity of soil mass in the same region does not vary greatly, but that of soil masses in different regions differs significantly, due to regional characteristics.

Acknowledgments This research was financially supported by projects of the National Natural Science Foundation (No.: 41272301 and No.: 40472139), the Ministry of Education (2012BAJ11B04), the Institute of Hydrogeology and Environmental Geology, and the Shijiazhuang Bureau of Science and Technology (No.: 121383A).

References

- Adrian OG, Rudolph LD, Cherry AJ (1999) Analysis of long-term land subsidence near Mexico City: field investigations and predictive modeling. *Water Resour Res* 35(11):3327–3341
- Di Prisco C, Imposimato S, Vardoulakis I (2000) Mechanical modeling of drained creep triaxial tests on loose sand. *Geotechnique* 50(1):73–82
- Garlanger JE (1972) The consolidation of soil exhibiting creep under constant effective stress. *Geotechnique* 22:71–78
- Hu RL (2004) Review on current status and challenging issue of land subsidence in China. *Eng Geol* 76:65–77
- Jia J, Wang JH, Lou XM, Xie XL, Liu CP (2009) The settlement characteristic of underground urban complex in Shanghai. *J Shanghai Jiaotong University Sci* 14(3):365–370
- Liu CH, Liao JJ, Huang CT, Ouyang S (2004) Characterization of land subsidence in the Chaoshui River alluvial fan Taiwan. *Environ Geol* 45:1154–1166
- Lubis AM, Sato T, Tomiyama N, Isezaki N, Yamanokuchi T (2011) Ground subsidence in Semarang-Indonesia investigated by ALOS-PALSAR satellite SAR interferometry. *J Asian Earth Sci* 40(5):1079–1088
- Oda M, Kazama H (1998) Microstructure of shear bands and its relation to the mechanisms of dilatancy and failure of dense granular soils. *Geotechnique* 48(4):465–481
- Sakiyan J, Yazicigil H (2004) Sustainable development and management of an aquifer system in western Turkey. *Hydrogeology J* 12:66–80
- Shamoto Y, Zhang JM, Goto S (1997) Mechanism of large post-liquefaction deformation in saturated sand. *Soils Found* 37(2):71–80
- Shi X, Xue Y, Wu J, Ye S, Yun Z et al. (2008) Characterization of regional land subsidence in Yangtze Delta, China: the example of Su-Xi-Chang area and the city of Shanghai. *Hydrogeol J* 16(3):593–607
- Liu S and Lin Y (2011) Introduction to Grey Systems Modeling Software. *Underst Complex Syst* 68:287–302
- Standard for soil test method (GB/T50123) (1999) The standard of the People's Republic of China, China Planning Press, Beijing 74–80 (in Chinese)
- Teatini P, Ferronato M, Gambolati G, Bertoni W, Gonella M (2005) A century of land subsidence in Ravenna Italy. *Environ Geol* 47:831–846
- The Writing Committee of Handbook of engineering geology (1993) Handbook of engineering geology (3). China Building Industry Press, Beijing, p 181(in Chinese)
- VLade Poul, Liu Chi-Tseng (1998) Experimental study of drained creep behavior of sand. *J Eng Mech* 124(8):912–920
- Wang XY, Liu CL, Zhang Y (2003) Laboratory tests for identification of critical water table. *Rock Soil Mech* 27(6):875–879 (in Chinese)
- Wang XY, Chen J, Sun L, Han SP, Fei YH, Wang JZ, Liu CL, Zhang Y (2011) Laboratory study on the relationship between soil mass deformation and water seepage in North China. *Environ Earth Sci* 64(8):2195–2201
- Wu FQ, Xi Hu, Gong MF, Liu JY, Ren AW (2010) Unloading deformation during layered excavation for the underground powerhouse of Jinping I Hydropower Station, southwest China. *Bull Eng Geol Environ* 69(3):343–351
- Zhang Y, Xue YQ, Wu JC, Ji-Chun Wu, Shi XQ, Yu J (2010) Excessive groundwater withdrawal and resultant land subsidence in the Su-Xi-Chang area China. *Environ Earth Sci* 61(6):1135–1143
- Zhuang YC, Xie KH (2005a) Study on one-dimensional consolidation of soil under cyclic loading and with varied compressibility. *J Zhejiang Univ Sci* 6A(2):141–147
- Zhuang YC, Xie KH (2005b) Study on one-dimensional consolidation of soil under cyclic loading and with varied compressibility. *J Zhejiang Univ Sci* 6A(2):141–147